

17 March, 1998

# Evidence for $\xi$ – and $t$ -dependent damping of the $\mathcal{P}$ omeron flux in the proton

Samim Erhan and Peter E. Schlein

University of California\*, Los Angeles, California 90095, USA.

## Abstract

We show that a triple-Regge parametrization of inclusive single diffraction agrees with the data in the following two domains: (a)  $\xi > 0.03$  at all  $t$ , (b)  $|t| > 1 \text{ GeV}^2$  at all  $\xi$ . Since the triple-Regge parametrization fails when applied to the full  $\xi$ – $t$  range of the total single-diffractive cross section, we conclude that damping occurs only at low- $\xi$  and low- $|t|$ . We give a (“toy”) parametrization of the damping factor,  $D(\xi)$ , valid at low- $|t|$ , which describes the  $d\sigma_{sd}^{total}/dt$  data at the ISR and roughly accounts for the observed  $s$ –dependence of  $\sigma_{sd}^{total}$  up to Tevatron energies. However, an effective damping factor calculated for the CDF fitted function for  $d^2\sigma_{sd}^{total}/d\xi dt$  at  $\sqrt{s} = 1800 \text{ GeV}$  and  $|t| = 0.05 \text{ GeV}^2$ , suggests that, at fixed- $\xi$ , damping increases as  $s$  increases.

We conjecture that, in the regions where the triple-Regge formalism describes the data and there is no evidence of damping, factorization is valid and the  $\mathcal{P}$ omeron-flux-factor may be universal. With the assumption that the observed damping is due to multi- $\mathcal{P}$ omeron exchange, our results imply that the recent UA8 demonstration that the effective  $\mathcal{P}$ omeron trajectory flattens for  $|t| > 1 \text{ GeV}^2$  is evidence for the onset of the perturbative 2-gluon pomeron. Our damping results may also shed some light on the self-consistency of recent measurements of hard-diffractive jet production cross sections in the UA8, CDF and ZEUS experiments.

submitted to Physics Letters B

---

\* Supported by U.S. National Science Foundation Grant PHY94–23142



# 1 Introduction

The inclusive (inelastic) production of beam-like particles, known as single diffraction, as in:

$$\bar{p} + p_i \rightarrow X + p_f + c.c. \quad (1)$$

and its analogous  $pp$  and  $ep$  interactions, presents one of the most interesting phenomena in strong interaction physics. An observed “rapidity gap” (absence of particles in a range of rapidity) between  $X$  and  $p_f$  in the final state signifies that the entire (color singlet) residual momentum of the proton, with beam momentum fraction,  $\xi = 1 - x_p$ , participates in the interaction between it and the second beam particle. This effect is described in terms of the exchange of the  $\mathcal{P}$ omeron Regge trajectory[1], which embodies the idea of “factorization”. The momentum transfer,  $t$ , and the beam momentum fraction,  $x_p$ , of the final state proton,  $p_f$ , “tag” the corresponding parameters of the exchanged  $\mathcal{P}$ omeron.

Since  $x_p \sim 1$  is observed to be the most likely beam momentum fraction of the final-state  $p_f$ , correspondingly the most likely value of the  $\mathcal{P}$ omeron’s momentum fraction in the proton,  $\xi$ , is near zero. Nonetheless, at current collider energies the squared-invariant-mass of the system  $X$  in Eq. 1,  $s' = \xi s$  to good approximation, can be quite large. This fact led to a proposal[2] to study hard scattering in such interactions, as a means of determining if the  $\mathcal{P}$ omeron possesses an observable partonic structure. The observation of the predicted hard scattering[3, 4, 5] supported the notion that the  $\mathcal{P}$ omeron behaves like a quasi-real object inside the proton with an effective  $\mathcal{P}$ omeron flux factor. An open question is to what extent such a flux factor is universal; for example, is it independent of beam particle or center-of-mass energy, or are there regions of phase space where factorization breaks down, due to interference with other more complex phenomena (e.g. multiple- $\mathcal{P}$ omeron-exchange) ?

One of the long-standing theoretical problems in high energy hadronic interactions has been the understanding of  $s$ -channel unitarization in  $\mathcal{P}$ omeron-exchange (diffractive) interactions. Empirically, one finds that the total diffractive cross section,  $\sigma_{sd}^{total}$ , in Reaction 1 and in the corresponding  $pp$  interaction, initially rises from threshold and tends to level off or “flatten” at high energy[6], whereas the dominant triple- $\mathcal{P}$ omeron[7] description of these processes (see below) continues to rise and soon exceeds the total  $p\bar{p}$  cross section. There is no built-in mechanism in the pure triple- $\mathcal{P}$ omeron process to account for the observed flattening of  $\sigma_{sd}^{total}$ , and hence avoid the violation of unitarity.

Figure 1 displays the problem [8–17]. The  $s$ -dependence of the total cross section for React. 1,  $\sigma_{sd}^{total}$  is shown<sup>1</sup> for Feynman- $x_p > 0.95$  (or  $\xi < 0.05$ ) of the final state proton or antiproton (the domain where  $\mathcal{P}$ omeron-exchange is dominant).  $\sigma_{sd}^{total}$  rises sharply from its threshold at 11.3 GeV beam momentum and gently levels off to  $\sim 9$  mb at the highest Fermilab energy. The solid curve in Fig. 1 is the triple-Regge prediction discussed below. At high energies, it is in complete disagreement with the measured cross section.

---

<sup>1</sup>It is conventional to quote  $\sigma_{sd}^{total}$  for  $\xi_{min} < \xi < 0.05$ , because the experimental acceptance usually depends weakly on  $x_p$  in this region and because the integrated background from non- $\mathcal{P}$ omeron exchange and other sources in this region is small enough to be neglected.

In the continuing theoretical efforts to satisfy  $s$ –channel unitarity [18–22], the words, screening, shadowing, absorption and damping are all used[23] to describe effects due to multiple  $\mathcal{P}$ omeron exchange (two- $\mathcal{P}$ omeron-exchange is also an important component in understanding  $pp$  elastic scattering[24] at low- $|t|$ ). These calculations have had varying degrees of success. Goulianos has taken a more pragmatic approach[6] to satisfying unitarity and suggested that the integral of the  $\mathcal{P}$ omeron flux factor in a proton should saturate at unity above  $\sqrt{s} \sim 22$  GeV.

In the present Letter, we find that damping is confined to the low- $\xi$ , low- $|t|$  region. We continue the analysis of the UA8 Collaboration[25] and demonstrate that there are regions either at larger  $\xi$  or at larger  $t$ , where the available data are well described by the triple-Regge formula and therefore require no damping.

It is thus clear that the damping function depends on both  $\xi$  and  $t$ . We attempt to determine the  $\xi$ –dependence at low- $|t|$  of an “effective” multiplicative damping factor which could account for the discrepancies between data and solid curve in Fig. 1. However, we call it a “toy damping factor” for several reasons. First, there are large gaps in the available data in Fig. 1 and some inconsistencies, therefore making it impossible to find a unique function. Secondly, the processes which give rise to the observed damping may imply a breakdown of factorization, in which case a simple universal damping factor may not exist at low- $\xi$  and low- $|t|$ . Finally, there is some evidence that the nature of the  $\xi$ –dependence may itself depend on  $s$  at our highest energies.

## 2 Triple–Regge phenomenology

We briefly summarize the relevant formula. The Mueller–Regge expansion[7] for the differential cross section of React. 1 is:

$$\frac{d^2\sigma_{sd}}{d\xi dt} = \sum_{ijk} G_{ijk}(t) \cdot \xi^{1-\alpha_i(t)-\alpha_j(t)} \cdot (s')^{\alpha_k(0)-1} \quad (2)$$

where  $\alpha_i(t)$  is the Regge trajectory for Reggeon  $i$ . The sum is taken over all possible exchanged Reggeons. The  $G_{ijk}(t)$  are products of the various Reggeon–proton and triple–Reggeon couplings and the signature factors.

There are two dominant terms in Eq. 2 at small  $\xi$ , namely  $ijk = \mathcal{P}\mathcal{P}\mathcal{P}$  and  $\mathcal{P}\mathcal{P}\mathcal{R}$ , where the first term corresponds to the triple- $\mathcal{P}$ omeron process, and the second corresponds to other non-leading,  $C=+$  trajectories (e.g.,  $f_2$ ) in the  $\mathcal{P}$ omeron–proton interaction. The  $\mathcal{P}\mathcal{P}\mathcal{P}$  term increases with increasing  $s'$ , whereas the  $\mathcal{P}\mathcal{P}\mathcal{R}$  term decreases with increasing  $s'$ .

Because the  $\mathcal{P}$ omeron is the highest–lying trajectory, when  $i = j = \mathcal{P}$ omeron,  $1 - 2\alpha$  is negative and the differential cross section increases sharply as  $\xi \rightarrow 0$ . This corresponds to the empirical observation that the most likely momentum fraction of the  $\mathcal{P}$ omeron in the proton,  $\xi$ , is near zero. Thus, the sharp rise in the triple–Regge prediction of  $\sigma_{sd}^{total}$  in Fig. 1 is due to the kinematic fact that the minimum value of  $\xi$  decreases with increasing  $s$  as  $\xi_{min} = s'_{min}/s$

For fitting to data, Eq. 2 has been rewritten[25] as:

$$\frac{d^2\sigma_{sd}}{d\xi dt} = [K F_1(t)^2 e^{bt} \xi^{1-2\alpha(t)}] \cdot \sigma_0 [(s')^{\epsilon_1} + R(s')^{\epsilon_2}], \quad (3)$$

where,

- the left-hand bracket is taken as the  $\mathcal{P}$ omeron flux factor,  $F_{\mathcal{P}/p}(t, \xi)$ , and the right-hand bracket (together with the constant,  $\sigma_0$ ) is the  $\mathcal{P}$ omeron–proton total cross section,  $\sigma_{\mathcal{P}p}^{total}$ .
- The two terms in  $\sigma_{\mathcal{P}p}^{total}$  correspond to the  $(s')^{\alpha_k(0)-1}$  factor<sup>2</sup> in the  $\mathcal{PPP}$  and  $\mathcal{PPR}$  terms in Eq. 2. Thus,  $\sigma_{\mathcal{P}p}^{total}$  has a form similar to that of real particle cross sections[26].
- The products  $K\sigma_0$  and  $K\sigma_0 R$  are, respectively, the values of  $G_{\mathcal{PPP}}(t)$  and  $G_{\mathcal{PPR}}(t)$  at  $t = 0$ .
- The  $\mathcal{P}$ omeron trajectory,  $\alpha(t)$ , has been shown[25] to become relatively flat for  $|t| > 1$  GeV<sup>2</sup> (see next section); therefore a quadratic term is added to the standard linear trajectory[24],  $\alpha(t) = 1.10 + 0.25 t + \alpha'' t^2$ . The non-zero value of  $b$  in  $e^{bt}$  compensates for the presence of the quadratic component in the  $\mathcal{P}$ omeron trajectory<sup>3</sup>.
- $|F_1(t)|^2$  is the standard Donnachie–Landshoff[24] form-factor.<sup>4</sup> Since it has never been shown to describe React. 1 at large  $t$ , the  $e^{bt}$  factor also serves as a possible correction. Thus, the product,  $|F_1(t)|^2 e^{bt}$ , carries the  $t$ -dependence of the  $G_{ijk}$  in Eq. 2 and is assumed to be the same for both  $G_{\mathcal{PPP}}$  and  $G_{\mathcal{PPR}}$ . Physically, this means that the  $\mathcal{P}$ omeron has the same flux factor in the proton, independent of whether the  $\mathcal{P}$ omeron–proton interaction proceeds via  $\mathcal{P}$ omeron–exchange or Reggeon–exchange.

### 3 Where is triple–Regge applicable ?

We already know from the information in Fig. 1 that the dominant contribution to the total cross section, namely the data with small– $\xi$  and small– $|t|$ , are not described by the triple–Regge formalism; a damping of the  $\mathcal{P}$ omeron flux with increasing  $s$  is certainly required in this region. However, we see no reason to suppose that the same damping must apply to the entire  $\xi$ – $t$  domain<sup>5</sup>, as proposed by Goulianos[6]. However, this issue

<sup>2</sup>At very large  $s'$ , rescattering effects may lead to a logarithmic dependence on  $s'$  as well as to other complications[23].

<sup>3</sup>If, as Donnachie and Landshoff[27] have suggested,  $\sigma_{\mathcal{P}p}^{total}$  depends on momentum transfer, that dependence would also be absorbed into the  $e^{bt}$  factor.

<sup>4</sup> $F_1(t) = \frac{4m_p^2 - 2.8t}{4m_p^2 - t} \cdot \frac{1}{(1-t/0.71)^2}$

<sup>5</sup> $\mathcal{P}$ omeron–exchange dominates out to  $\xi \sim 0.05$  and contributes significantly to  $\xi \sim 0.1$ .

can be resolved by using available data to determine if there are regions in the  $\xi$ – $t$  plane where the formalism does apply; that is, where damping is not required.

The UA8 collaboration has recently reported[25] a (successful) simultaneous fit of Eq. 3 to their data on React. 1 at  $\sqrt{s} = 630$  GeV and the extensive data sample of the CHLM collaboration at the CERN–ISR with  $\sqrt{s} = 23.5$  and 30.5 GeV. They use the values,  $\alpha_k(0) - 1 = 0.10$  and -0.32, obtained for the  $\mathcal{P}$ omeron and  $f/A2$  trajectories, respectively, in fits to real–particle total cross sections[26, 28, 29].

The four free parameters,  $K\sigma_0$ ,  $\alpha''$ ,  $b$  and  $R$ , are determined by fitting Eq. 3, plus an empirical background function of the form,  $Ae^{ct}\xi^1$ , to the combined ISR–UA8 data set in the range<sup>6</sup>,  $\xi = 0.03$ –0.10. The fitted parameters are:

$$\begin{aligned} K\sigma_0 &= 0.72 \pm 0.10 \quad \text{mb GeV}^{-2} \\ \alpha'' &= 0.079 \pm 0.012 \quad \text{GeV}^{-4} \\ b &= 1.08 \pm 0.20 \quad \text{GeV}^{-2} \\ R &= 4.0 \pm 0.6 \end{aligned}$$

This value of  $\alpha''$  was independently confirmed[25] in fits to the  $\xi$ –dependence in the peak region with  $\xi < 0.03$ .

These triple–Regge results can be used to predict the total cross section of React. 1,  $\sigma_{sd}^{total}$ , by integrating Eq. 3 over the entire  $t$ –range, as well as for  $\xi_{min} < \xi < 0.05$ . This yields the solid curve in Fig. 1 and illustrates the discrepancy[6] with the experimental  $\sigma_{sd}^{total}$ .

Fig. 2 from Ref. [25] shows the ISR[30] and UA8 data[25] data in the restricted region,  $0.03 < \xi < 0.04$ , where the small ( $\sim 15\%$ ) non– $\mathcal{P}$ omeron–exchange background can be ignored (the background is smaller than the size of the dots in the figure and about the same magnitude as the systematic uncertainty in absolute cross sections). The similarity of  $\frac{d^2\sigma}{d\xi dt}$  at  $\xi = 0.035$  at both ISR and  $Spp\bar{S}$  energies reflects the fact that  $\sigma_{\mathcal{P}p}^{total}(s')$  has nearly the same value at both  $\sqrt{s'} = 5$  and 118 GeV.<sup>7</sup> The term,  $(s')^{-0.32}$ , in Eq. 3 makes this possible. The solid curves in Fig. 2 are fits to these data *without a background term* and yield values of the 4 parameters which are in excellent agreement<sup>8</sup> with those given above from the  $\xi = 0.03$ –0.10 fit, thus lending credence to the reliability and stability of the fits.

We have found a second region in the  $\xi$ – $t$  plane, at small– $\xi$  but large– $|t|$ , where the triple–Regge formalism also describes the ISR and UA8 data — with no additional free parameters. Fig. 3 shows the high momentum–transfer part of  $\sigma_{sd}^{total}$  for  $\xi_{min} < \xi < 0.05$  and the limited  $|t|$ –range, 1.0–2.0 GeV<sup>2</sup>, plotted vs.  $s$  for the ISR and UA8 data. The solid curve is the prediction of Eq. 3 using the above parameters. The dashed curve is

<sup>6</sup>For  $\xi > 0.03$ , there are no concerns about experimental resolution causing “spill–over” from the large peak at  $\xi \sim 0$ .

<sup>7</sup>This arises because, at fixed  $\xi$  and  $t$  in Eq. 3,  $\frac{d^2\sigma}{d\xi dt}$  is proportional to  $\sigma_{\mathcal{P}p}^{total}(\xi s)$ .

<sup>8</sup>The same four parameters from this fit are  $(0.67 \pm 0.08)$ ,  $(0.078 \pm 0.013)$ ,  $(0.88 \pm 0.19)$  and  $(5.0 \pm 0.6)$ , respectively.

obtained by decreasing the  $b$ -parameter by  $1\sigma$  from its central value. We see that, in contrast with the situation for  $\sigma_{sd}^{total}$ , the triple-Regge formula, Eq. 3, accounts for the observed  $s$ -dependence of the total single diffractive cross section in the high- $|t|$  range, 1.0–2.0 GeV $^2$ . The different shapes of the curves in Figs. 1 and the solid curve in Fig. 3 are due to the  $t$ -dependence of the  $\mathcal{P}$ omeron trajectory.

We have thus demonstrated that damping depends on both  $\xi$  and  $t$ ; it only exists in the small- $\xi$ , small- $|t|$  region, and is not required by data away from that region — either at larger  $\xi$  or at larger  $|t|$ . This could explain why CDF[17] reports abnormally large backgrounds in triple- $\mathcal{P}$ omeron fits to their (low- $\xi$ , low- $|t|$ ) data at  $\sqrt{s} = 1800$  GeV. For example, at  $\xi = 0.035$  (and  $|t| = 0.05$  GeV $^2$ ) where normally 15–20% background is found, their fitted formula corresponds to non- $\mathcal{P}$ omeron-exchange backgrounds of 51%. Such a result can be expected if a  $\xi$ -dependent Damping factor is required, but is left out of the fit; the fitted (large) background term compensates for the wrong  $\xi$ -dependence in the triple-Regge equation without damping. Since CDF only reports the fitted functions, we compare our prediction of  $\frac{d^2\sigma}{d\xi dt}$  with the sum of their “signal” and “background” terms. This sum corresponds to the solid bands in Fig. 4; the curves are the  $\frac{d^2\sigma}{d\xi dt}$  vs.  $t$  predictions of Eq. 3 at  $\xi = 0.035$ . We see that, at 1800 GeV, the prediction agrees to within  $1\sigma$  of the CDF result; at 546 GeV, there is also good agreement at the lowest  $|t|$ -value, although their fitted  $t$ -dependences at the two energies are not self-consistent.

## 4 Empirical determination of damping at small $(\xi, t)$

The  $t$ -dependence of the disagreement between triple-Regge and the measured cross section is best seen by comparing the predictions with the experimental values of  $d\sigma_{sd}^{total}/dt$  plotted vs.  $t$ . This is done in Figs. 5 for eight ISR energies<sup>9</sup> and in Fig. 6 at the SppS-Collider<sup>10</sup>.

The dashed and dotted curves in Figs. 5 and 6 are the (undamped) triple-Regge predictions for  $d\sigma/dt$ , calculated by integrating Eq. 3 over the range,  $\xi_{min} < \xi < 0.05$  (for the dotted curve,  $b$  is decreased by  $1\sigma$  from its central value).

At the ISR energies, where the triple-Regge prediction only exceeds the data by about 10–15% (see Fig. 1), the differences between dashed curves and data in Fig. 5 are hardly noticeable, because the dot sizes are roughly similar to the discrepancies. At  $\sqrt{s} = 630$  GeV, however, the same effect is larger and highly visible. At that energy, we see that there is a gradual transition from the low- $|t|$  region which dominates  $\sigma_{sd}^{total}$ , and where the experimental  $\sigma_{sd}^{total}$  is smaller than the (undamped) triple-Regge prediction, to the higher- $|t|$  region where the predictions agree with the data. This seems to be a smooth transition over the  $|t|$ -range, 0.5–1.0 GeV $^2$ . The situation at the lower ISR energies in Figs. 5 is similar but less pronounced. We conclude that the discrepancies between predictions and data are confined to the low- $|t|$  region.

---

<sup>9</sup>Some of these data were obtained with unequal energies for the two beams

<sup>10</sup>The UA4 points come from two independent runs, one at high- $\beta$  and one at low- $\beta$  which allowed them to span most of the available  $t$ -range.

Since, as noted above, the calculated rise in  $\sigma_{sd}^{total}$  with increasing  $s$  is due to the fact that, kinematically,  $\xi_{min}$  decreases with increasing  $s$ , it seems natural to introduce an empirical damping factor,  $D(\xi)$ , in Eq. 3 which suppresses small  $\xi$ -values; *i.e.*, we strike at the “heart” of the problem.  $D(\xi)$  will be unity everywhere except at small- $\xi$ .

For  $D(\xi)$ , we have tried a “toy” damping function which decreases from unity for  $\xi < 0.008$ , following a quadratic function as shown in Fig. 7. The parameters of the quadratic function are chosen to reproduce the leveling-off of  $\sigma_{sd}^{total}$  at ISR energies in Fig. 1. To account for the Tevatron and  $Spp\bar{S}$  points, an additional (steep) fall-off is needed for  $\xi < 0.0002$ . We arbitrarily use a cubic form<sup>11</sup>. The dashed curves on Fig. 1 shows how such a function accounts reasonably well<sup>12</sup> for  $\sigma_{sd}^{total}$  at high energies.

The solid curves in Figs. 5 and 6 are calculated from Eq. 3 multiplied by the above damping factor. As expected from Fig. 1, the effect of damping is very small at ISR energies, but increases with  $s$ . At the energy of the  $Spp\bar{S}$ , however, the damping is about a factor of 3 in the low  $t$  region, which dominates  $\sigma_{sd}^{total}$ . There is good agreement with the damping predictions at low- $|t|$  in both Figs. 5 and 6.

While, as explained above, the parameters of the quadratic term are chosen to agree with the departure of the ISR cross sections from the triple-Regge prediction in Fig. 1, there seems to be no reason a-priori why this formulation should be valid at higher energies. To clarify this point, we assume that the formula CDF fitted[17] to their data is a sufficient description of  $\frac{d^2\sigma}{d\xi dt}$  and compare its  $\xi$ -dependence at  $|t| = 0.05$  GeV<sup>2</sup> with that of Eq. 3. The band in Fig. 7 shows the ratio of the CDF  $\frac{d^2\sigma}{d\xi dt}$  at 1800 GeV to the triple-Regge prescription, which can be interpreted as an empirical damping factor. This decreases from near unity at  $\xi = 0.03$  to about 0.5 at  $\xi = 0.01$ , but is insufficient to account for the factor of  $\sim 5$  required by the 1800 GeV cross section in Fig. 1; therefore an additional (rapid) decrease in the damping factor must occur at smaller  $\xi$ , analogous to our toy damping factor discussed above.

The CDF function thus indicates that, at larger  $s$ , the onset of damping occurs at increasingly larger  $\xi$ -values. However, this does not invalidate the solid (damped) curve calculated with the above  $D(\xi)$  and shown in Fig. 6, because the overall damping calculation is not sensitive to the details of  $D(\xi)$  in the larger  $\xi$ -region.

## 5 Conclusions

We first summarize the key points of this Letter:

- We have a triple-Regge parametrization of inclusive single diffraction which agrees with the data in two domains of the  $\xi-t$  plane: (a)  $\xi > 0.03$  at all  $t$ , (b)  $|t| > 1$  GeV<sup>2</sup> at all  $\xi$  (Figs. 2, 3 and 4). Since the triple-Regge parametrization fails when applied

<sup>11</sup> $D(\xi) = 7000\xi - (2.86 \cdot 10^7)\xi^2 + (3.62 \cdot 10^{10})\xi^3$ .  $D(\xi)$  has a total of 3 free parameters, since the quadratic and cubic have identical slopes and magnitudes at  $\xi = 0.0002$ . These were chosen to be the parameters of the quadratic function and the slope of the cubic function at  $\xi = 0$ .

<sup>12</sup>The bump between the ISR and  $Spp\bar{S}$  energies is due to the interplay between the 2-component  $\sigma_{pp}^{total}$  and the damping function at  $\xi_{min}$ .

to the full  $\xi-t$  range of the total single diffractive cross section ( $\xi_{min} < \xi < 0.05$  and all  $t$ ), we can conclude that damping occurs only at low- $\xi$  and low- $|t|$ .

- We have given a parametrization of the damping factor,  $D(\xi)$ , valid for  $t < 0.5 \text{ GeV}^2$ , which describes all the low- $|t|$   $d\sigma_{sd}^{total}/dt$  data at the ISR and roughly accounts for the observed  $s$ -dependence of  $\sigma_{sd}^{total}$  up to Tevatron energies (Figs. 1, 5, 6 and 7).
- An effective damping factor calculated for the CDF fitted function for  $\frac{d^2\sigma}{d\xi dt}$  at  $\sqrt{s} = 1800 \text{ GeV}$  and  $|t| = 0.05 \text{ GeV}^2$ , suggests that, at fixed- $\xi$ , damping increases as  $s$  increases (Fig. 7).

These results raise a number of issues: We can conjecture that, in the regions where the triple-Regge formalism describes the data and there is no evidence of damping, factorization is valid and the  $\mathcal{P}$ omeron-flux-factor may be universal. A systematic program of testing universality of the flux factor in these regions should be carried out in  $pp$ ,  $p\bar{p}$  and  $ep$  interactions.

Our damping results may shed some light on the measurements of the  $fK$  quantity from the cross sections for diffractive jet production in React. 1 and its analogue  $ep$  reaction ( $K$  is the normalization constant in Eq. 3 and  $f$  measures violation of the momentum sum rule, when  $f \neq 1$ ). Assuming that the  $\mathcal{P}$ omeron has dominant gluonic structure[31], there are three measurements of  $fK$ :

UA8 [5]	$fK = 0.30 \pm 0.10$
CDF [32]	$fK = 0.11 \pm 0.02$
ZEUS [33]	$fK = 0.37 \pm 0.15$

The fact that the UA8 data is at large- $|t|$  where there is no damping, whereas the CDF data is at small- $|t|$  where the damping factor in the region of the jets is of order 0.50, could account for the difference between the UA8 and CDF  $fK$  values.

In addition, despite the large errors, it is interesting that the UA8 and ZEUS values for  $fK$  are consistent. This might be expected, if there is no damping in  $ep$  collisions at high- $Q^2$ . Of course, at low- $Q^2$ , where the photon exhibits hadronic properties, multi- $\mathcal{P}$ omeron exchange, and hence damping, may result in smaller values of  $fK$ .

In order to further study the possible  $s$ -dependence of the effective damping factor, it would be very useful to make detailed measurements of single diffraction in  $pp$  interactions at RHIC energies. This would fill in the large gap between ISR and  $Spp\bar{S}$ -collider energies seen in Fig. 1.

We note that UA8[25] offers as possible explanations of their observed flattening of the  $\mathcal{P}$ omeron trajectory for  $|t| > 1 \text{ GeV}^2$ , either that it is an effect of multiple- $\mathcal{P}$ omeron exchange, or that it is evidence for the onset of the perturbative 2-gluon pomeron[34, 35]. In view of our observation that damping is not required in this  $t$ -region, it seems that the perturbative  $\mathcal{P}$ omeron, explanation is more likely. It may therefore be interesting to study the  $\gamma$ - $\mathcal{P}$ omeron cross section from  $t_{min}$  up through the  $|t| > 1 \text{ GeV}^2$  region.

## Acknowledgements

We thank A. Kaidalov, P. Landshoff and E. Gotsman for helpful comments.

## References

- [1] For reviews, see e.g.:  
A.B. Kaidalov, Phys. Reports 50 (1979) 157;  
G. Alberi and G. Goggi, Phys. Reports 74 (1981) 1;  
K. Goulianos, Phys. Reports 101 (1983) 169.
- [2] G. Ingelman and P.E. Schlein, Phys. Lett. B 152 (1985) 256.
- [3] R. Bonino et al. (UA8 Collaboration), Phys. Lett. B 211 (1988) 239.
- [4] A. Brandt et al. (UA8 Collaboration), Phys. Lett. B 297 (1992) 417.
- [5] A. Brandt et al. (UA8 Collaboration), Phys. Lett. B 421 (1998) 395.
- [6] K. Goulianos, Phys. Lett. B358 (1995) 379; B363 (1995) 268.
- [7] A.H. Mueller, Phys. Rev. D2 (1970) 2963; D4 (1971) 150;  
A.B. Kaidalov et al., Pisma JETP 17 (1973) 626;  
A. Capella, Phys. Rev. D8 (1973) 2047;  
R.D. Field and G.C. Fox, Nucl. Phys. B80 (1974) 367;  
D.P. Roy and R.G. Roberts, Nucl. Phys. B77 (1974) 240.
- [8] V. Blobel et al., Nucl. Phys. B92 (1975) 221.
- [9] H. Bialkowska et al., Nucl. Phys. B110 (1976) 300.
- [10] J.W. Chapman et al., Phys. Rev. Lett. 32 (1974) 257; the cross section at 405 GeV is multiplied by a factor 0.82 to estimate the value for  $x_p > 0.95$ .
- [11] S.J. Barish et al., Phys. Rev D9 (1974) 2689; Phys. Rev. Lett. 31 (1973) 1080.
- [12] F.T. Dao et al., Phys. Lett. B45 (1973) 399.
- [13] M.G. Albrow et al., Nucl. Phys. B108 (1976) 1.
- [14] J.C.M. Armitage et al., Nucl. Phys. B194 (1982) 365.
- [15] M. Bozzo et al. (UA4 Collaboration), Phys. Lett. B136 (1984) 217.
- [16] D. Bernard et al. (UA4 Collaboration), Phys. Lett. B186 (1987) 227.
- [17] F. Abe et al. (CDF Collaboration), Phys. Rev. D50 (1994) 5535.
- [18] A. Capella, J. Kaplan and J. Tran Thanh Van, Nucl. Phys. B 105 (1976) 333.
- [19] A.B. Kaidalov, L.A. Ponomarev and K.A. Ter-Martirosyan, Sov. J. Nucl. Phys. 44 (1986) 468.
- [20] P. Aurenche et al., Phys. Rev. D 45 (1992) 92.

- [21] E. Gotsman, E.M. Levin and U. Maor, *Zeit. Phys. C* 57 (1993) 667; *Phys. Rev. D* 49 (1994) R4321; *Phys. Lett B* 353 (1995) 526.
- [22] A. Capella, A. Kaidalov, C. Merino and J. Tran Thanh Van, *Phys. Lett. B* 337 (1994) 358.
- [23] A. Kaidalov, private communication (1998).
- [24] A. Donnachie & P.V. Landshoff, *Nucl. Phys. B* 231 (1984) 189; *Nucl. Phys. B* 267 (1986) 690.
- [25] A. Brandt et al. (UA8 Collaboration), *Nucl. Phys. B* 514 (1998) 3.
- [26] A. Donnachie & P.V. Landshoff, *Phys. Lett. B* 296 (1992) 227.
- [27] A. Donnachie & P.V. Landshoff, *Nucl. Phys. B* 244 (1984) 322.
- [28] J.R. Cudell, K. Kyungsik and K.K. Sung, *Phys. Lett. B* 395 (1997) 311; J.R. Cudell, K. Kang and S.K. Kim, “Simple Model for Total Cross Sections”, preprint, Brown–HET–1060, January 1997.
- [29] R.J.M. Covolan, J. Montanha & K. Goulianos, *Phys. Lett. B* 389 (1996) 176.
- [30] M.G. Albrow et al., *Nucl. Phys. B* 54 (1973) 6; M.G. Albrow et al., *Nucl. Phys. B* 72 (1974) 376.
- [31] C. Adloff et al. (H1 Collaboration), *Z. Phys. C* 76 (1997) 613.
- [32] F. Abe et al. (CDF Collaboration), *Phys. Rev. Lett.* 79 (1997) 2636.
- [33] M. Derrick et al. (ZEUS Collaboration), *Phys. Lett.* 356 (1995) 129.
- [34] L. Frankfurt and M. Strikman, *Phys. Rev. Lett.* 63, (1989) 1914; 64 (1990) 815.
- [35] J.C. Collins, L. Frankfurt and M. Strikman, *Phys. Lett. B* 307 (1993) 161.

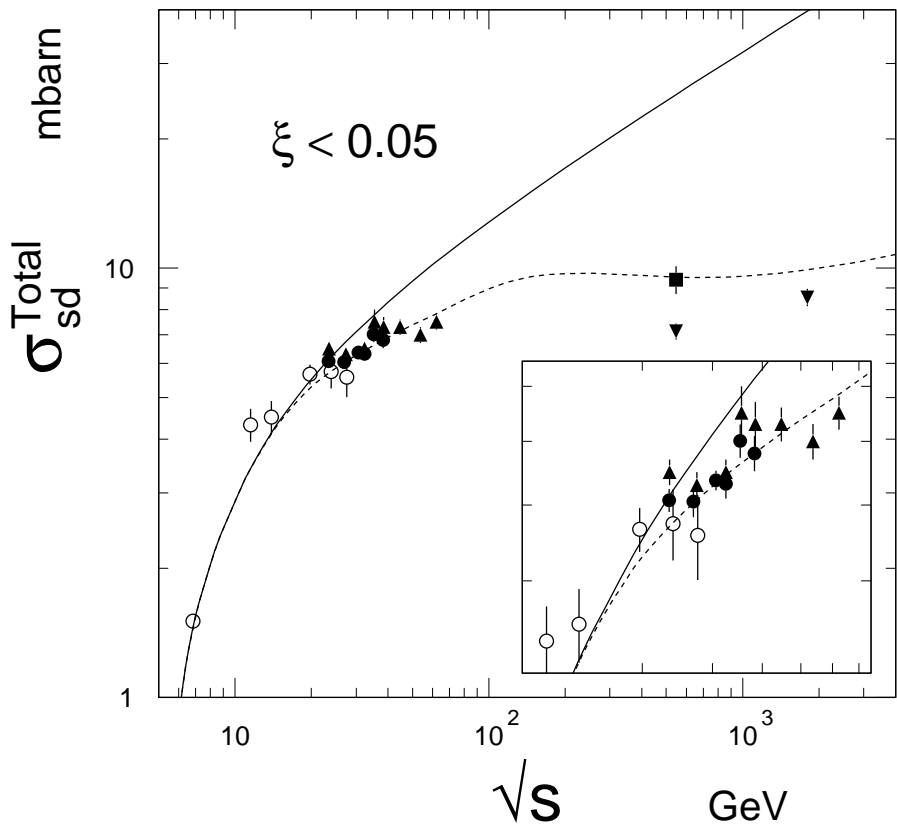


Figure 1:  $\sigma_{sd}^{total}$  of  $pp$  or  $p\bar{p}$  interactions (with  $\xi < 0.05$ ) vs.  $\sqrt{s}$  demonstrating the flattening of the cross section with energy (a factor of two is included to account for both hemispheres). The insert is a blow-up of the ISR energy range. The upper curve is the Triple-Regge prediction described in the text; the dashed curve shows the consequence of multiplying it by the “toy” damping factor discussed in the text. The lowest energy points (open circles) are from bubble chamber experiments [8–12]; followed by those from the ISR (solid circles[13] and triangles[14]), the  $SppS$ -Collider (solid square [15, 16]) and the Tevatron (inverted triangles [17]).

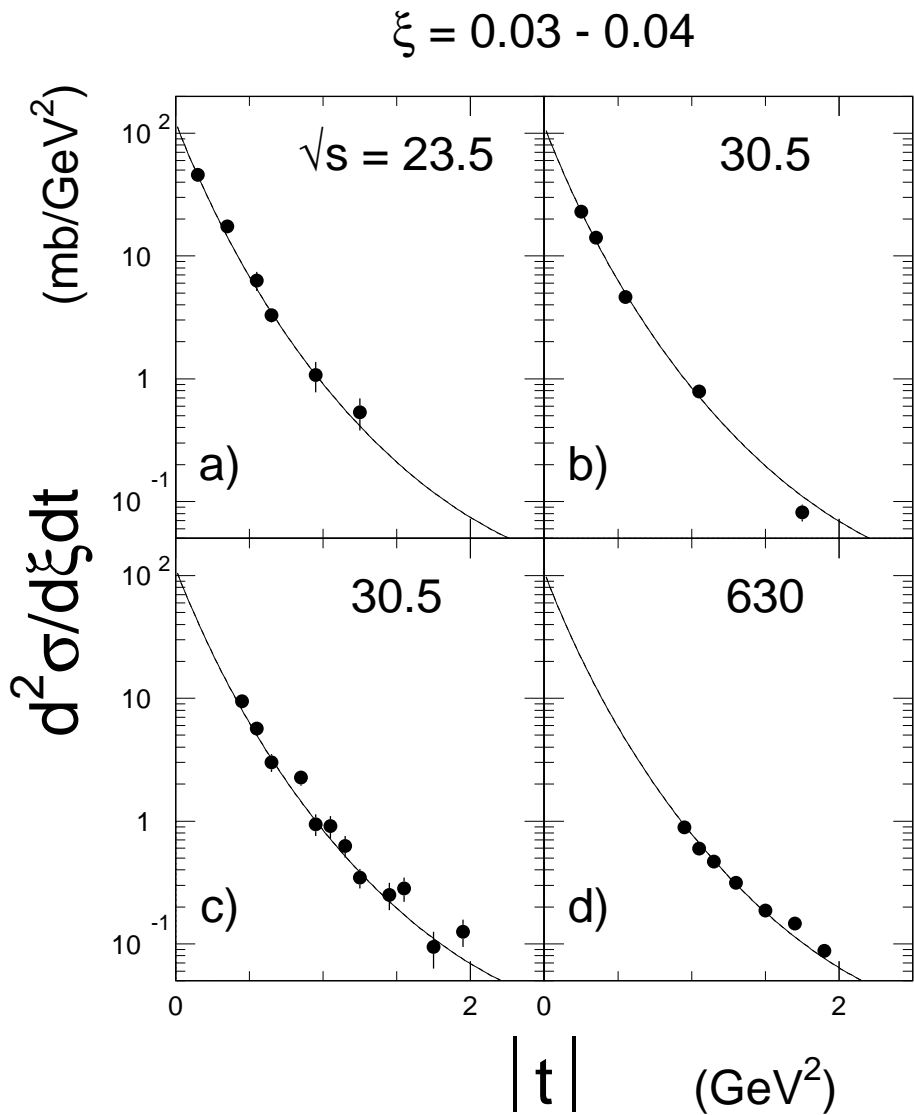


Figure 2: Differential cross section,  $\frac{d^2\sigma}{d\xi dt}$ , vs  $t$ , for 3 ISR measurements[30] and UA8[25] (single-arm cross sections). The curves correspond to the fit described in the text [25]. The points are averages of data in the  $\xi$ -range 0.03–0.04 (the non-Pomeron-exchange background in the data points is about the same magnitude as the diameter of the dots).

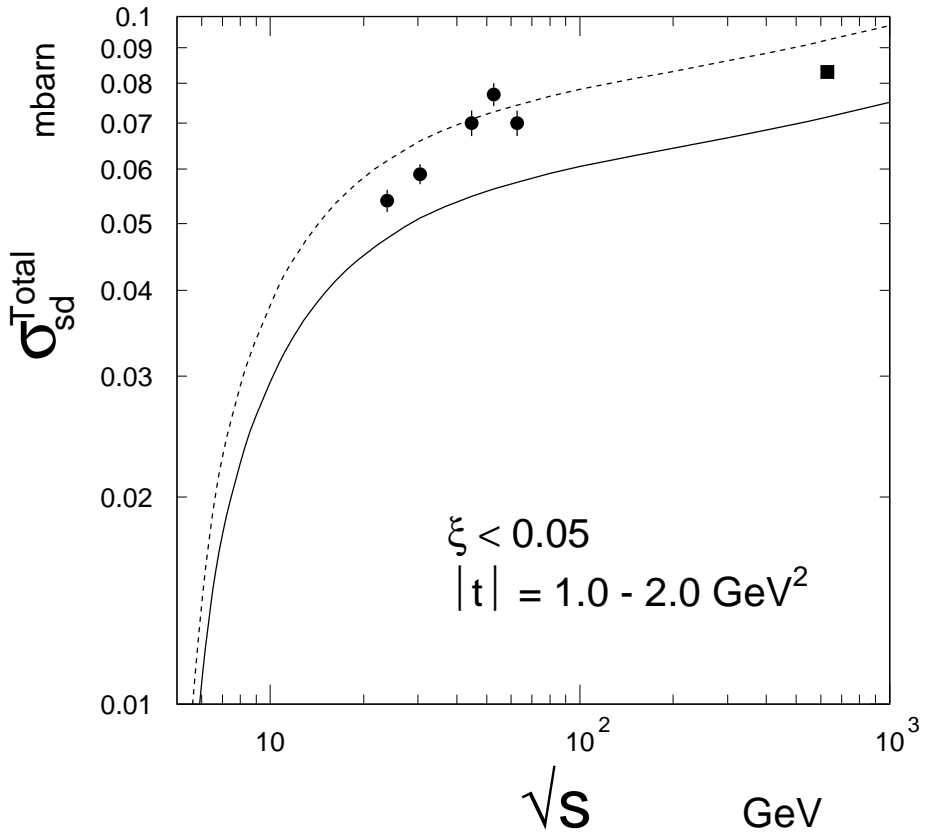


Figure 3:  $\sigma_{sd}^{total}$  for  $\xi < 0.05$  and  $|t| = 1.0 - 2.0 \text{ GeV}^2$  vs.  $\sqrt{s}$  (a factor of two is included to account for both hemispheres). The solid curve is the same Triple-Regge prediction used in Fig. 1 (where it is integrated over all  $t$ ); the dashed curve is the same, but with the “ $b$ ”-parameter decreased by  $1\sigma$  from its central value. The lowest energy points (closed circles) are from the ISR [13]; the highest energy point (solid square) is from the Sp $\bar{p}$ S-Collider [25]

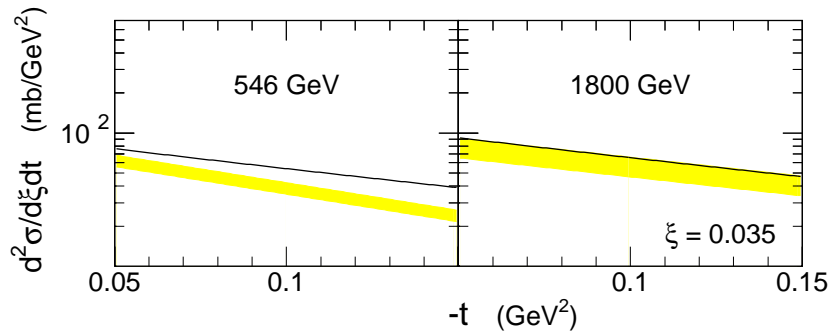


Figure 4: Bands are the CDF differential cross sections at  $\xi = 0.035$ , calculated from their fitted functions[17] (single-arm cross sections); the band widths are  $\pm 1\sigma$  errors on their amplitudes (as explained in the text, their “signal” and “background” are added together). The curves are from the same calculations used for the curves in Fig. 2.

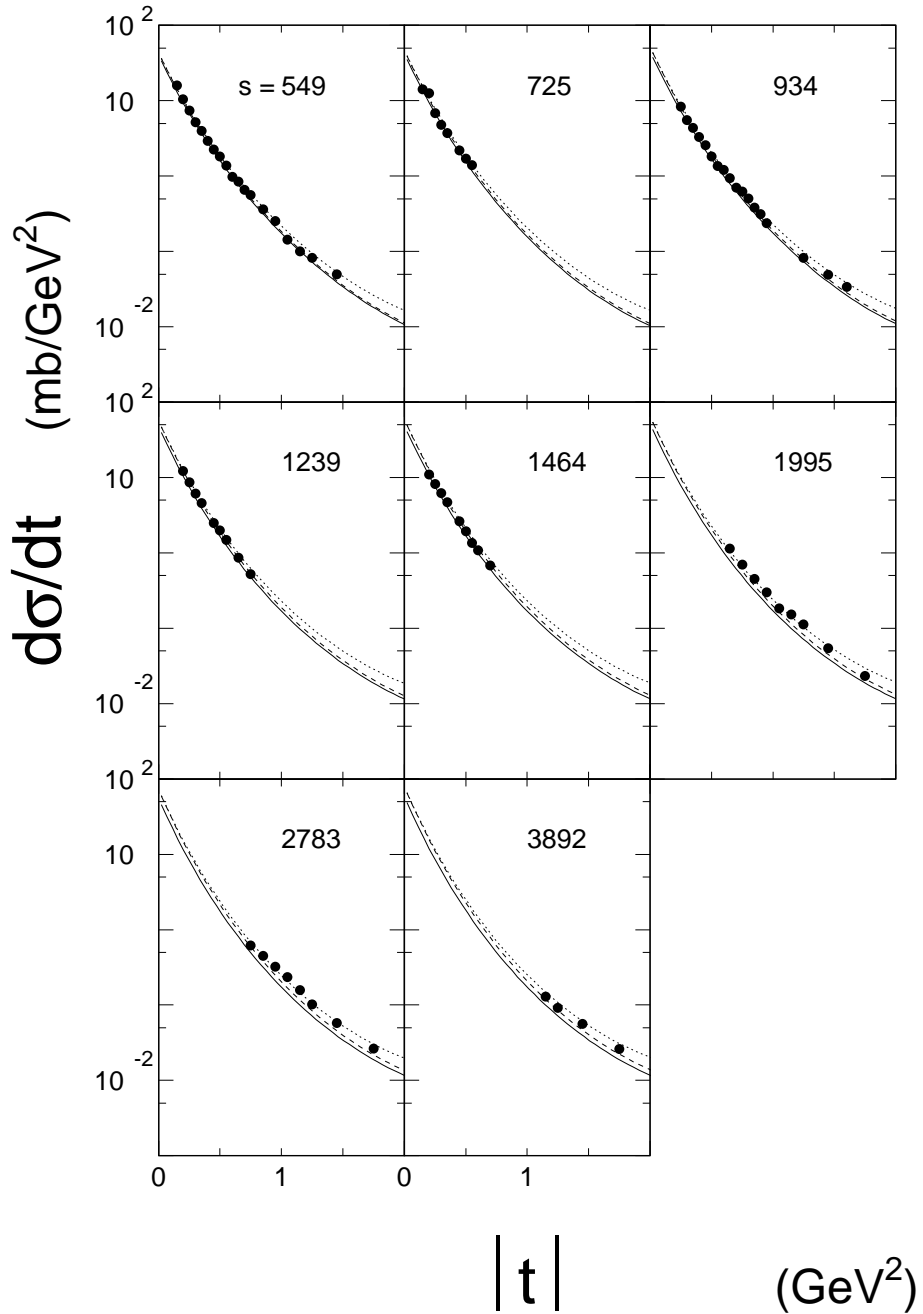


Figure 5:  $d\sigma/dt$  vs.  $|t|$  (single-arm cross sections) with  $\xi < 0.05$  at eight ISR[13, 14] energies. The numbers shown in each plot are their  $s$  values ( $\text{GeV}^2$ ). The solid curves are the integrals of Eq. 3 with damping included, using the parameters given in the text. The dashed and dotted curves are calculated without damping; the dashed curve uses the central value of  $b$ , while for the dotted curve,  $b$  is decreased by  $1\sigma$  from its central value.

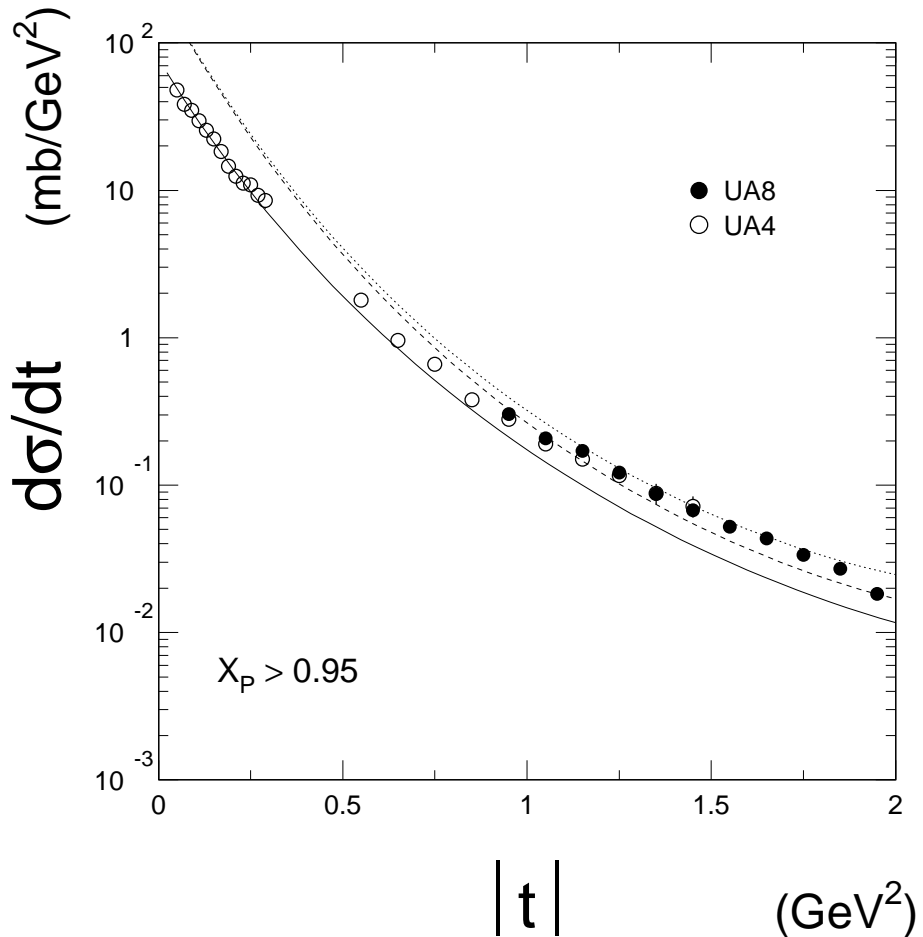


Figure 6: Inclusive differential cross section for protons in React. 1 for  $x_p > 0.95$ , measured in experiment UA8 with  $\sqrt{s} = 630$  GeV. and in experiment UA4[15, 16] with  $\sqrt{s} = 546$  GeV (single-arm cross sections; the integral is  $4.7 \pm 0.35$  mb, or  $9.4 \pm 0.7$  mb for  $\sigma_{sd}^{total}$ ). The solid curve is the integral of Eq. 3 with damping included, as explained in the text. The dashed and dotted curves are calculated without damping; the dashed curve uses the central value of  $b$ , while for the dotted curve,  $b$  is decreased by  $1\sigma$  from its central value.

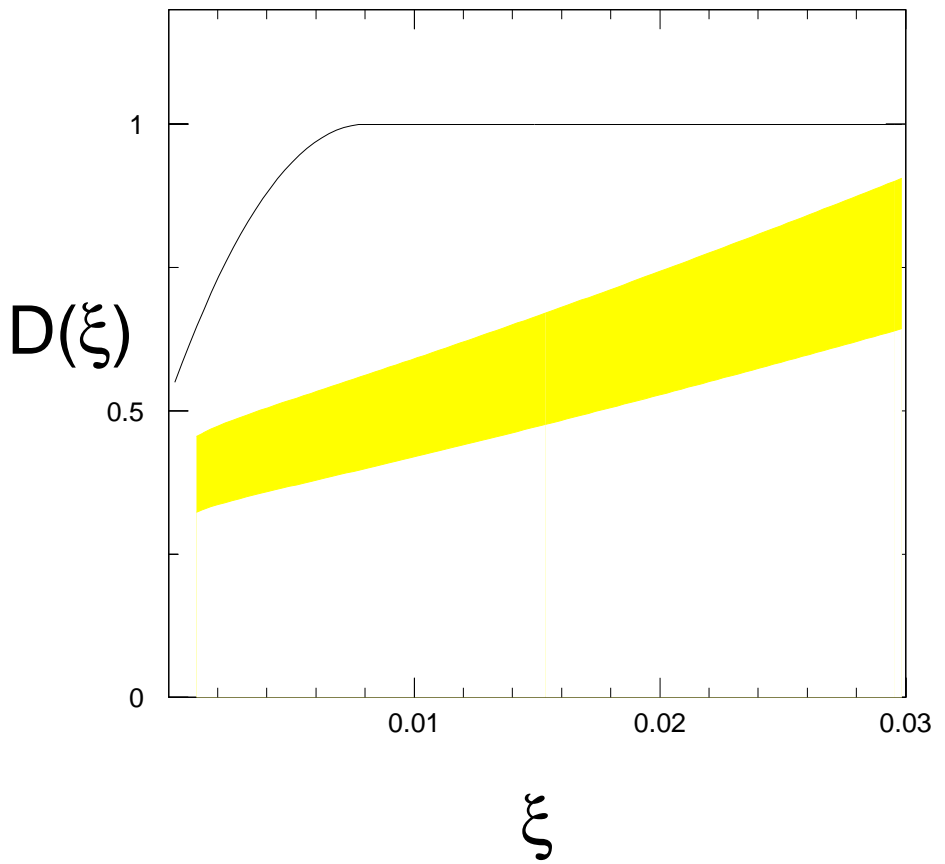


Figure 7: The damping function referred to in the text. In the  $\xi$ -range, 0.0002–0.008, the function shown is a quadratic,  $D(\xi) = 1 - 7500(0.008 - \xi)^2$ . For  $\xi < 0.0002$ , the function is made to drop quickly to zero following a cubic function, as described in the text. The band is the ratio of the CDF  $\frac{d^2\sigma}{d\xi dt}$  at  $|t| = 0.05$  GeV $^2$  and  $\sqrt{s} = 1800$  GeV to the triple-Regge prediction described in the text.